Preprints of the 19th World Congress
The International Federation of Automatic Control
Cape Town, South Africa. August 24-29, 2014

Longitudinal Manoeuvre Load Control of a Flexible Large-Scale Aircraft

L. Burlion * **C. Poussot-Vassal** * **P. Vuillemin** * **M. Leitner** ** **T. Kier** **

* *Onera - The French Aerospace Lab, F-31055 Toulouse, France.*
** *DLR, Institute of Robotics and Mechatronics, 82234, Wessling, Germany.*

Abstract: This paper discusses the design and validation of an integrated long range flexible aircraft load controller, at a single flight/mass configuration. The contributions of the paper are in twofold: *(i)* first, a very recent frequency-limited model approximation technique is used to reduce the dimension of the large-scale aeroservoelastic aircraft model over a finite frequency support while guaranteeing optimal mismatch error, secondly, *(ii)* a structured controller is designed using an $\mathcal{H}_\infty$-objective and coupled with an output saturation strategy to achieve flight performance and load clearance, *i.e.* wing root bending moment saturation. The entire procedure - approximation and control - is finally assessed on the high fidelity large-scale aircraft model, illustrating the effectiveness of the procedure on a high fidelity model, used in the industrial context in the load control validation process.

Keywords: Aircraft modelling, Model approximation, Load control, Output saturation

1. INTRODUCTION

1.1 Motivations and aircraft load control framework

The many different objectives flexible aircraft should fulfill (*e.g.* flight performances, load protection, noise reduction, etc.) render the controller design and tuning tasks very complex. Traditionally, these objectives are - reasonably - dissociated to each others, allowing to treat each flexible (modal) contribution separately [1], *e.g.* flight dynamics, then loads, then vibrations (see *e.g.* Gardonio (2002)). However, following efforts from structure and material engineers in lightning the aircraft mass in order to reduce the overall fuel consumption and gas emissions (*e.g.* fuselage and wing), the modal behaviour of each flexible modes and aerodynamical delays is likely to blend each other. More specifically, in the *load control* context, the first aeroelastic load mode might appears in low frequencies and interfere with the aircraft flight (rigid) dynamics.

As a matter of consequence, a control approach consists to design the flight and load controllers in a unified step, to both guarantee *(i)* good flight performances in *normal cruise situations* and *(ii)* load preservation when *strong manoeuvre or gust disturbance occur* to guarantee that load upper and lower limitations are never reached. The load control is a critical step in the aircraft validation since aircraft manufacturer must guarantee the authorities that critical loads are monitored in all situations, whatever the manoeuvre is (see also Gaulocher et al. (2007); Haghighat et al. (2012)).

Moreover, it is worth mentioning that the aeroservoelastic models involved in the design and validation procedures of such a controller take into account the flight physics, the aeroelastic phenomenon (structural loads, unsteady aerodynamic loads and delays) and the flight control system behaviour. Consequently, the resulting linear state-space models, representing the aircraft at frozen flight / mass configuration, are of large-scale (state vector of order n around 2000). Even if each model can always be questioned or amended, this large amount of variables comes with an enhanced accuracy, but also renders the control design and optimization tasks even more complex.

This paper reports original results obtained within the joint collaboration between Onera and DLR, on the development of advanced methodologies for load control design applied to a complex flexible large-scale aircraft model, at one single load dimensioning flight and mass configuration. More specifically, with reference to Figure 1, the paper is attached to approximate the large-scale model $\mathbf{H}$ (blue block) and, grounded on the low-order model $\hat{\mathbf{H}}$, design a dedicated flight and load control law that should fulfil flight performance in normal situations and prevent load limitations *i.e.* saturations, when critical manoeuvre occurs (red blocks).

Designing such a controller, involving large-scale dynamical model, is a challenging problem (Gadient et al. (2012)), indeed:

- the large number of states involved in the dynamical model results in computational complexity,
- the load preservation specifications are given as strong time-domain constraints on the wing root bending moment ($WRM_x(t)$), an output of the model,
- the nominal flight control law performances, when no critical load are detected, must be ensured (*e.g.* load

[1] Even if in practice iterative re-tuning is required.

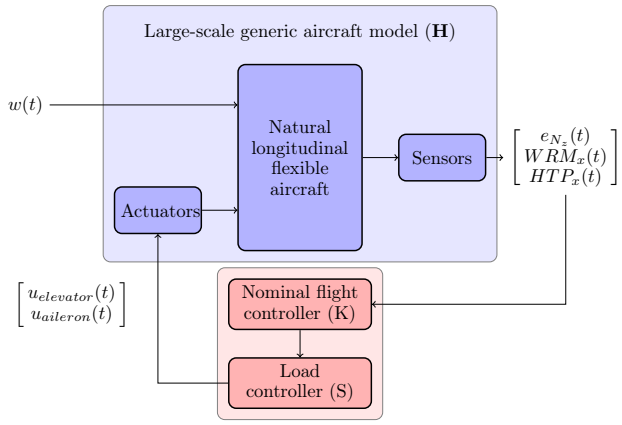

Fig. 1. Flexible aircraft model ($\mathbf{H}$) and load controller.

factor $N_z(t)$ should tracks its reference $N_z^*(t)$, thus $\mathbf{lim}_{t\to\infty} e_{N_z}(t) = 0$, $e_{N_z}(t) = N_z(t) - N_z^*(t)$), and,
- high frequency flexible - lightly - damped modes must remain stable, and unmodified.

1.2 Paper notations and structure

The flexible aircraft modelling and approximation steps are briefly described in Section 2. Then, Section 3 describes the core contribution, *i.e.* a combined flight and load control strategy, allowing to provide *good flight quality while preserving load saturation*. The complete validation of the proposed load control is performed on the full order flexible aircraft model, using flight certification criterion, assessing the interest and effectiveness of the proposed controller. Conclusions are given in Section 4.

Throughout the paper, the following notations will be used: $\mathbf{H}$ (*resp.* $H(s)$) denotes the full order state-space model realization (*resp.* transfer function, which is a $\mathcal{H}_p^{n_y\times n_u}$ matrix complex-valued function [2]) of order n and $\hat{\mathbf{H}}$ (*resp.* $\hat{H}(s)$) stands for the reduced order state-space model realization (*resp.* transfer function) of order $r \ll n$. Given the matrices $M = \begin{bmatrix} M_{11} & M_{12} \\ M_{21} & M_{22} \end{bmatrix}$ and K of suitable dimensions, $\mathcal{F}_l(M,K)_{w\to z} = M_{11} + M_{12}K(I - M_{22}K)^{-1}M_{21}$ denotes the transfer from w to z of the lower linear fractional transformation operator that interconnects M with K.

2. LARGE-SCALE LONG RANGE FLEXIBLE AIRCRAFT MODELLING, APPROXIMATION AND PROBLEM FORMULATION

2.1 Large-scale modelling

The considered dynamical aircraft model, represents a longitudinal long range generic aircraft, linearised at varying mass and flight configurations (mass, flight altitude and speed). This model is obtained by merging the mass and geometry of the aircraft (*e.g.* obtained from finite element mapping) using a flexible tool for simulation of loads analysis models (see Hofstee et al. (2003)), with method and equations of integrating gust and manoeuvre models (see Kier and Looye (2009)). The entire procedure is made available through the use of FlightDynLib, an integrated tool (see Looye et al. (2005)). When combined with flight, load and aerodynamical delays dynamical equations, a complete integrated model is thus generated at different flight configurations.

In this study, *one single* linear large-scale dynamical model, valid at one single mass/flight configuration will be considered. The resulting aeroservoelastic model form includes the aeroelastic model coupled to the load recovery (see Figure 1). This system can be represented by its transfer function $H(s) = C(sI_n - A)^{-1}B + D$, or equivalent state-space realization $\mathbf{H}$ as:

$$\mathbf{H} : \begin{cases} \dot{x}(t) &= Ax(t) + Bu(t) \\ y(t) &= Cx(t) + Du(t) \end{cases}, \tag{1}$$

where $A \in \mathbb{R}^{n\times n}$, $B \in \mathbb{R}^{n\times n_u}$, $C \in \mathbb{R}^{n_y\times n}$ and $D \in \mathbb{R}^{n_y\times n_u}$ (with $n \approx 1700$, $n_u = 3$ and $n_y = 3$ are the number of states, inputs and outputs, respectively). In the considered application, the input vector is composed of

- $w(t)$, the external disturbance input representing a gust impact on the entire wing and fuselage,
- $u_{elevator}(t)$ and $u_{aileron}(t)$, representing elevator and outer aileron equivalent control surfaces action,

and the output vector is composed of

- $N_z(t)$, the vertical load factor, representing the *flight dynamic performance*,
- $WRM_x(t)$, the wing root bending moment, which is the value to be monitored to ensure *load saturation preservation* (this value represents the effort at the fuselage/wing connection and is thus dimensioning for safety certification purpose),
- $HTP_x(t)$, the root bending moment at the tail of the aircraft, which should be monitored as well (but the variable is not load-dimensioning).

2.2 $\mathcal{H}_2$-optimal model approximation

As the original system is of large-scale ($n \approx 1700$), the application of the standard control optimization tools is no longer adapted for numerical and memory management reasons. This is why an open-loop model approximation step is firstly done (see Antoulas (2005)). Since the aim of model approximation is to construct a reduced-order model $\hat{\mathbf{H}}$ (or $\hat{H}(s)$) that captures the main original system dynamics input/output behaviour while preserving stability, the $\mathcal{H}_2$-norm mismatch error is often addressed (see Gugercin et al. (2008)). More specifically, in the applicative context of - load - control, it is more convenient to consider the mismatch error over a limited frequency range (*e.g.* the range on which the control law will act). This consideration has been addressed in recent model approximation results through the use of the frequency-limited $\mathcal{H}_2$-norm, denoted $\mathcal{H}_{2,\Omega}$-norm (Ω stands for the frequency support). The resulting approximation problem consists of seeking an approximation $\hat{H}(s)$ of $H(s)$, so that

$$\hat{H} := \arg \min_{\substack{G \in \mathcal{H}_\infty^{n_y\times n_u} \\ \mathbf{rank}(G) = r \ll n}} ||H - G||_{\mathcal{H}_{2,\Omega}}. \tag{2}$$

[2] the $\mathcal{H}_p^{n_y\times n_u}$ denotes the set of $n_y \times n_u$ matrix-valued complex-valued functions $H(s)$ with component $h_{ij}(s)$ that are analytic in the open right half-plane $\mathbb{C}^+$, and wher the $||.||_{\mathcal{H}_p}$-norm is defined.

Beside the fact that problem (2) is non convex, some algorithm have been proposed to solve it, reaching the so-called first order optimality conditions, ensuring that a local (hopefully global) optimum is reached. In this paper context, the aircraft model described above has been approximated using different reduction techniques. Figure 2 reports the $\mathcal{H}_{2,\Omega}$-norm mismatch approximation error (Ω = [0 100]Hz) as a function of the order of the approximated model r, using either the best MATLAB [3] method, the **ISTIA** proposed in Poussot-Vassal (2011) and extended in Vuillemin et al. (2013) and **DARPO**, a Descent Algorithm for Residues and Poles Optimization of Vuillemin et al. (2014).

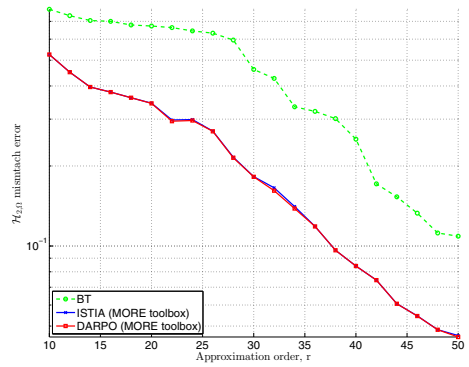

Fig. 2. $\mathcal{H}_{2,\Omega}$-norm mismatch error as a function of the order r of the approximated model for: **BT** (green rounded line) and **ISTIA** of the MORE toolbox (blue crossed line) and **DARPO** of the MORE toolbox (red solid squared line).

With reference to Figure 2, it is clear that the **ISTIA** and **DARPO** provide better approximated models over the bounded frequency support than the standard **BT** and will thus be preferred in the following. Without loss of generality, from now on, when $\hat{\mathbf{H}}$ (or $\hat{H}(s)$) is mentioned, it will refer to approximated model of order $r = 50$ obtained with the **DARPO**, providing an relative error of $\approx 4\%$.

Remark 1. (Model approximation). As it is not the topic of the paper, the **ISTIA** and **DARPO** methods are not described here. However, interested reader may refer to the MORE toolbox for additional details [4].

2.3 Performance specifications and constraints

At the considered dimensioning mass and flight configuration, as stated in the Section 1, let us formalize the performance and constraints as follows:

FQ1 **Flight qualities 1 (frequency domain)**: ensure load tracking, *i.e.* $N_z(t)$ should follow $N_z^*(t)$ reference.

LP1 **Load performances 1 (frequency domain)**: ensure wind root bending moment ($WRM_x(t)$) attenuation in low frequency until the first load mode, in response to wind disturbance, with negligible impact on higher modes. This performance is also evaluated through a frequency-limited $\mathcal{H}_2$-norm improvement,

$$100\ \frac{|\mathcal{J}^{\text{nom}} - \mathcal{J}|}{\mathcal{J}^{\text{nom}}}, \tag{3}$$

where $\mathcal{J}^{\text{nom}} = ||T_{w\to WRM_x}||_{\mathcal{H}_{2,[0.1\ 100]}}$ without control, and $\mathcal{J} = ||T_{w\to WRM_x}||_{\mathcal{H}_{2,[0.1\ 100]}}$ when the controller is connected.

LP2 **Load performance 2 (time domain)**: ensure that the wing root bending moment $WRM_x(t)$ remains within lower and upper limits, critic for load clearance,$WRM_x^{min} \leq WRM_x(t) \leq WRM_x^{max}$.

Const1 **Controller constraints (frequency domain)**: the control should not act above 10Hz in order to not deteriorate lightly damped flexible modes.

Const2 **Structural constraints (structure)**: the controller should have a simple structure. Moreover, it is likely for aircraft engineers to dissociate the nominal law with le load clearance one, as illustrated in Figure 1.

Note that item **LP2** is a very far to be a trivial task since it cannot be handled in an efficient way through linear approaches. It is why in the next section, a dedicated load controller will be added to the nominal flight control to monitor the wing root bending moment and guarantee that the limitations are kept.

3. MANOEUVER-LOAD ALLEVIATION CONTROLLER DESIGN

3.1 (Nominal) flight controller design (K)

To achieve flight and load control performances in nominal situation (when no wing root bending moment limitations are reached), *i.e.* to address objectives **FQ1** and **LP1**, while ensuring constraints **Const1** and **Const2**, a linear structured controller is designed with $\mathcal{H}_\infty$-norm minimization objective, as

$$K := \arg \min_{\substack{C \in \mathcal{H}_2^{n_u \times n_y} \\ \mathbf{rank}(C) = n_c}} ||\mathcal{F}_l^\star(\hat{H}, C)||_{\mathcal{H}_\infty}, \tag{4}$$

where, to avoid $\mathcal{H}_\infty$-norm cross minimization transfer, $\mathcal{F}_l^\star(\hat{H}, C)$ is structured as,

$$\mathcal{F}_l^\star(\hat{H}, C) = \mathbf{diag}\Big(\begin{array}{l} W_i\mathcal{F}_l(\hat{H}, C)_{N_z^*\to e_{N_z}} W_o, \\ W_i\mathcal{F}_l(\hat{H}, C)_{w\to e_{N_z}, WRM_x, HTP_x} W_o, \\ W_i\mathcal{F}_l(\hat{H}, C)_{N_z^*, w\to u_{aileron}, u_{elevator}} W_o \Big), \end{array} \tag{5}$$

where W_i and W_o are the weighting function classically used in frequency controller synthesis to address **FQ1** and **LP1** objectives. Without loss of generality and with reference to (4), to address *(i)* **Const1**, the controller is structured such that the control rolls-off above 10Hz and enforcing the controller to belong $\mathcal{H}_2^{n_u \times n_y}$, and *(ii)* **Const2**, by imposing a rank constraint on the controller. This is achieved through used of standard algorithm made available by Apkarian and Noll (2006) (see Figure 3).

3.2 Output saturation design of the wing root bending moment $WRM_x(t)$

Additionally - and this is the specificity of the treated problem to handle the fact that the wing root bending mo-

[3] In most of the case the best result is obtained when using the Balanced Truncation (**BT**) method.

[4] Webpage `http://w3.onera.fr/more` Poussot-Vassal and Vuillemin (2012).

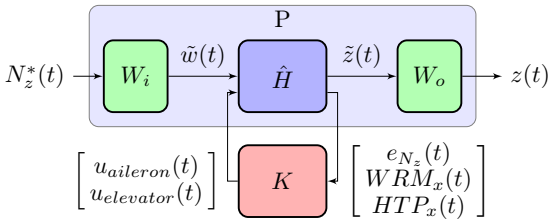

Fig. 3. Flexible aircraft model ($\hat{H}$), weighting filters (W_i, W_o) and load controller (K).

ment must remain inside a specified interval (*e.g.* for structural limitations purpose) an output saturation constraint must be specified (**LP2**). Mathematically, it consists in guaranteeing $WRM_x^{\min} < WRM_x(t) < WRM_x^{\max}$. In the following, this specificity is treated through a reformulation of the output saturation into an input saturation one, on which a performance-oriented controller will be applied. Note that the objective of the load saturation is to alleviate loads at the wing/fuselage location. However, to achieve flight performance, loads still have to be maintained elsewhere on the aircraft. Consequently, the objective is to balance the load of the WRM_x to the elevator surface HTP_x. Therefore, in what follows, the actuator ensuring the output saturation will be the elevator ($u_{elevator}$), only. The proposed approach does not require any on-line optimization procedure, unless standard approaches based on predictive control (Haghighat et al. (2012)).

3.3 Output to input saturation transform (S)

General result: The general method which consists in converting an interval constraint on an output $z(t)$ into a saturation on the control law $u(t)$ is described in Burlion (2012). The first step consists in computing the relative degree (denoted $d_u^{rel}(z)$) of the constrained output $z(t)$ with respect to the control value $u(t)$. In the context of the paper, we have $d_{u_{elevator}}^{rel}(WRM_x) = 0$, which means that the value of $u_{elevator}$ instantaneously changes the value of WRM_x.

Proposition 1. (OIST). Let us assume $z = WRM_x$ and the wind disturbance w to be measured and let us note (where $B_{WRM,u_e} \neq 0$)

$$\begin{aligned} &WRM_x\dot{\hat{x}}(t) = C_{WRM_x}\hat{x}(t) + B_{WRM_x,w}w(t) \\ &+B_{WRM_x,u_a}u_{aileron}(t) + B_{WRM_x,u_e}u_{elevator}(t), \quad (6) \end{aligned}$$

and

$$\begin{cases} WRM_x^{\min}(\hat{x}, w, u_{aileron}) = WRM_x^{\min} - C_{WRM_x}\hat{x} \\ -B_{WRM_x,w}w - B_{WRM_x,u_a}u_{aileron} \\ \\ WRM_x^{\max}(\hat{x}, w, u_{aileron}) = WRM_x^{\max} - C_{WRM_x}\hat{x} \\ -B_{WRM_x,w}w - B_{WRM_x,u_a}u_{aileron} \end{cases}.$$

In the simple case of relative degree 0, the Output to Input Saturation Transform (**OIST**) (Burlion (2012),Burlion and de Plinval (2013)) boils down saying that

$$\begin{cases} \forall t \geq 0, \quad B_{WRM,u_e}u_{elevator}(t) \in \\ \left[WRM_x^{\min}(\hat{x}, w, u_{aileron}), WRM_x^{\max}(\hat{x}, w, u_{aileron})\right] \end{cases}$$

then,

$$\forall t \geq 0, \quad WRM_x(t) \in [WRM_x^{\min}, WRM_x^{\max}]$$

providing the state $\hat{x}(t)$ remains stable when $u_{elevator}(t)$ saturates.

One remarks that the output interval constraint has been replaced by a saturation on $u_{elevator}$ whose bounds are time varying and depend on the internal state and on the other inputs.

In the relative degree $d_{u_{elevator}}^{rel}(WRM_x) = 0$, the method is rather simple but requires that the internal state x remains stable when the control law saturates. This proposition is closely related to the stability of the zeros associated to the transfers whose output is WRM_x since it is necessary that the zero dynamics associated to the output WRM_x remain stable when the constraint is activated. In the considered benchmark, the transfer functions $WRM_x(s)/u_{elevator}(s)$, $WRM_x(s)/u_{aileron}(s)$ and $WRM_x(s)/w(s)$ unfortunately possess unstable zeros and it is then not possible to apply the input saturation which is obtained through the application of Proposition 1.

Relaxation of the method by approximating the non minimum phase constrained output: The application of this saturation on $u_{elevator}(t)$ ensures that $WRM_x(t)$ remains inside its interval.

To alleviate this limitation, we propose to relax our saturation function by considering a saturation on an approximation of $WRM_x(t)$ instead of a saturation on $WRM_x(t)$. Let us note $WRM_x^{approx}(t)$ this new output: it must be close enough to $WRM_x(t)$ to have very similar bounds but must be a minimum phase.

The transfer functions from the inputs to $WRM_x(t)$, exhibits zeros in the right half plane whith high magnitude. Therefore we propose to remove them in this stable plane by changing their real value sign (see Figure 4). Associated to these new transfer functions, we obtain a new output, namely WRM_x^{approx} which is minimum phase and whose behavior is very close to the original non minimum phase output WRM_x. This is not so surprising since moving the zeros leads to bad effects since they have relatively large real value in our model values. Indeed, for instance moving a given pure real zero named $a \gg 0$, means that the ratio between the approximated transfer function and the original one is:

$$\frac{a-s}{a+s} \approx e^{-\frac{2}{a}s},$$

according to the well known Padé's first order approximation method, this ratio means there is approximately a delay between the outputs and its value is thus very small ($\frac{2}{a} \ll 1$). Finally, the controlled input saturation is based on a minimum phase output of the same system and noting:

$$\begin{aligned} &WRM_x^{approx}(t) = C_{WRM}^{approx}x^{approx}(t) + B_{WRM,w}^{approx}w(t) \\ &+B_{WRM,u_a}^{approx}u_{aileron}(t) + B_{WRM,u_e}^{approx}u_{elevator}(t), \quad (7) \end{aligned}$$

we finally saturate our elevator control law accordingly *i.e.*

$$\begin{cases} \forall t \geq 0, \quad B_{WRM,u_e}^{approx}u_{elevator}(t) \in \\ \left[WRM_x^{\min,approx}(t), WRM_x^{\max,approx}(t)\right] \end{cases}. \quad (8)$$

3.4 Large-scale numerical validation

In order to validate the proposed approach, a commonly used certification scenario in aeronautics to assess the manoeuvre load control, will be used and applied on

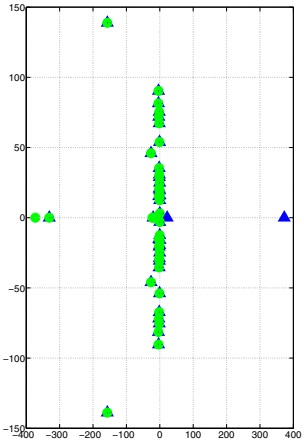

Fig. 4. Illustration of the approximation: the zeros of the transfer $WRM_x(s)/u_{elevator}(s)$ (*resp.* $WRM_x^{approx}(s)/u_{elevator}(s)$) are plotted in blue triangle (*resp.* in green round).

the large-scale model. This scenario, called "Manoeuvre Vertical Stretched" (MVS), consists in considering the aircraft flying at 1g and applying the following stick trajectory: *(i)* push the pilot stick with a sine shape until a load factor of 2.5g is reached, then *(ii)* released to turn back to 1g with a sine like function (see black solid line on Figure 5 top middle frame). The main objectives and results are reported on Figure 5.

With reference to the left frames, the frequency responses from the wind to the controlled outputs are reported. One can first notice that the closed-loop responses (solid red) with respect to the open-loop ones (dashed blue) are attenuated in low frequency and at the first resonance pick around 3Hz, while higher frequencies (above 10Hz) are not modified thanks to the controller structure that rolls-off above 10Hz. When considering the middle frames, the time responses to a MVS are reported. These frames compare the responses either with (solid red) or without (dashed blue) the load clearance controller presented in Section 3.3. First, top frame illustrates the fact that the load factor $N_z(t)$ reference is well tracked with both controller. The only slight difference occurs at $t = 10$s and $t = 15$s when the wing root bending moment is saturated (middle frame). Indeed, as illustrated in the middle frame, the proposed load saturation control allows to prevent limitation overshoot, maintaining the wing root bending moment within load limitations. This is a strong property and very important for certification purpose since it allows to guarantee that, whatever the exogenous input, the load envelope is preserved. Indeed, the nominal flight control is not able to prevent saturation without a significant diminution of the flight performances.

To quantify the effectiveness of the anti-load controller, the attenuation metric (3) indicates a gain of 25% in load attenuation, which is very encouraging for further developments. Finally, bottom right frame shows the control signal, illustrating the smoothness of the control law, even in saturation situations, which is a demand from aircraft engineers.

4. CONCLUSIONS AND PERSPECTIVES

In this paper, a strategy for manoeuvre load control has been presented and validated on a large-scale high fidelity model, constructed to faithfully reproduce the flexible aircraft behaviour at one single flight point. The proposed control design is based on a frequency-limited model approximation, followed by an innovative structured controller linked with an appropriate output saturation mechanism. This output saturation mechanism recast a controls input saturation one, allows to use the nominal controller and ensures good flight performance in most of the case, while guaranteeing wing root bending moment limitation only when it is necessary. Both frequency and time domain results emphasize the effectiveness of the proposed structure. Forthcoming work will address the robustness property by considering additional flight points/mass.

ACKNOWLEDGEMENT

The research leading to these results has received funding from the European Union's Seventh Framework Program (FP7/2007-2013) for the Clean Sky Joint Technology Initiative under grant agreement CSJU-GAM-SFWA-2008-001.

REFERENCES

Antoulas, A.C. (2005). *Approximation of Large-Scale Dynamical Systems*. Advanced Design and Control, SIAM, Philadelphia.

Apkarian, P. and Noll, D. (2006). Nonsmooth $\mathcal{H}_\infty$ Synthesis. *IEEE Transaction on Automatic Control*, 51(1), 71–86.

Burlion, L. (2012). A new saturation function to convert an output constraint into an input constraint. In *Proceedings of the 20th Mediterranean Conference on Control and Automation*, 1211–1216.

Burlion, L. and de Plinval, H. (2013). Keeping a ground point in the camera field of view of a landing uav. In *Proceedings of the IEEE International Conference on Robotics and Automation*, 5763–5768.

Gadient, R., Lavretsky, E., and Wise, K. (2012). Very Flexible Aircraft Control Challenge Problem. In *Proceedings of the AIAA Guidance, Navigation, and Control Conference*. Minneapolis, Minnesota, USA.

Gardonio, P. (2002). Review of Active Techniques for Aerospace Vibro-Acoustic Control. *Journal of Aircraft*, 39(2), 206–214.

Gaulocher, S., Roos, C., and Cumer, C. (2007). Aircraft load alleviation during maneuvers using optimal control surface combinations. *AIAA Journal of Guidance, Control and Dynamics*, 30(2), 591–600.

Gugercin, S., Antoulas, A.C., and Beattie, C.A. (2008). $\mathcal{H}_2$ Model Reduction for Large Scale Linear Dynamical Systems. *SIAM Journal on Matrix Analysis and Applications*, 30(2), 609–638.

Haghighat, S., Liu, H., and Martins, J. (2012). A model predictive gust load alleviation controller for a highly flexible aircraft. *Journal of Guidance, Control and Dynamics*.

Hofstee, J., Kier, T., Cerulli, C., and Looye, G. (2003). A Variable, Fully Flexible Dynamic Response Tool for

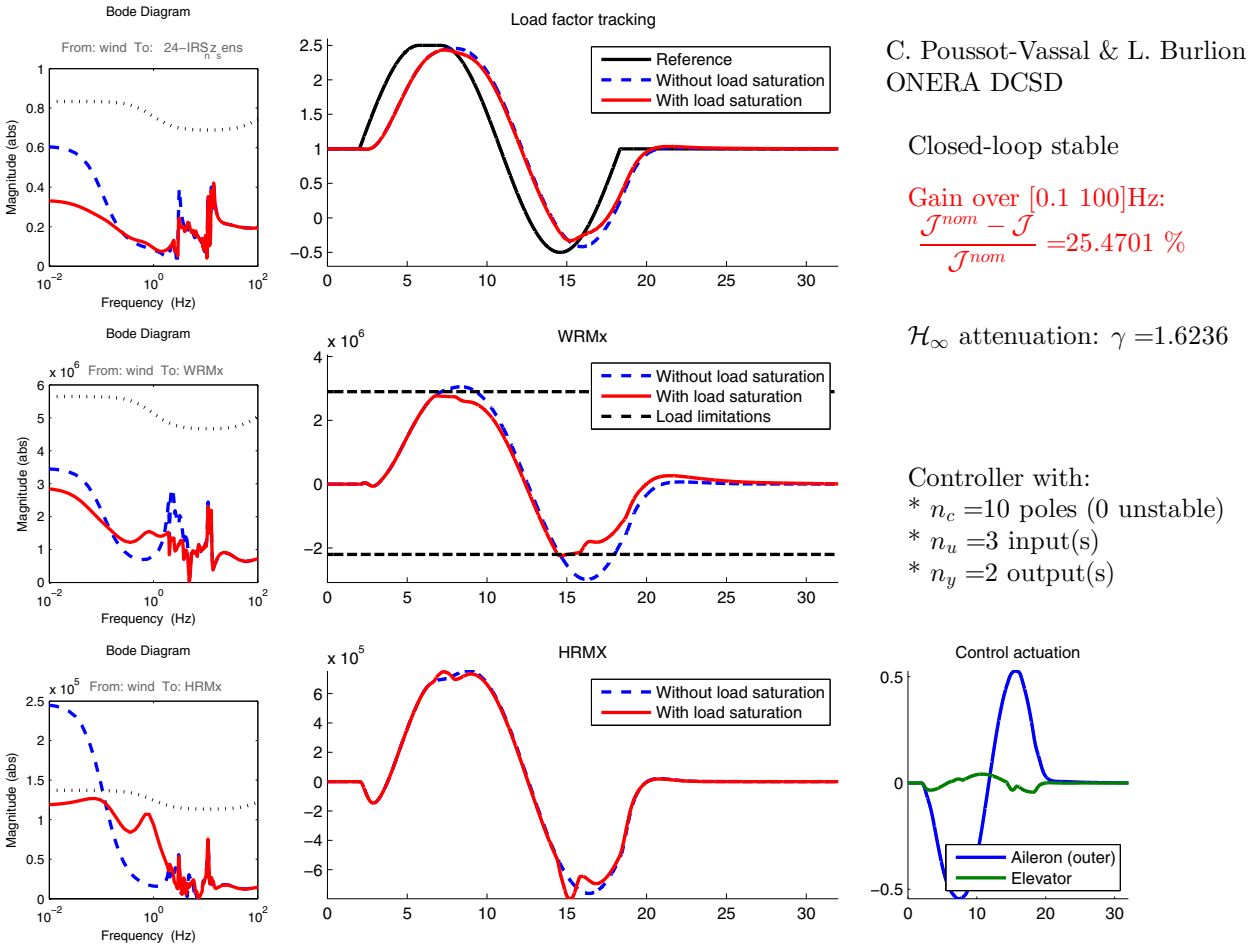

Fig. 5. Control results, applied on the large-scale flexible aircraft model. Left frames: frequency domain responses of the load factor (N_z), wing root bending moment (WRM_x) and tail root bending moment (HTP_x) in response to a wind disturbance (w) - open-loop: dashed blue, closed-loop: solid red, weighting filter used in the synthesis: dotted black. Middle frames: time domain behaviour in response to the MVS. Top frame: load factor tracking; Middle frame: wing root bending moment; and Bottom frame: HTP behaviour. Right side: attenuation criteria, property of the controller and control signal of the controller with load saturation.

Special Investigations (VarLoads). In *International Forum on Aeroelasticity and Structural Dynamics*.

Kier, T. and Looye, G. (2009). Unifying Manoeuvre and Gust Loads Analysis. In *International Forum on Aeroelasticity and Structural Dynamics*, IFASD-2009-106.

Looye, G., Hecker, S., Kier, T., and Reschke, C. (2005). FlightDynLib: An Object-Oriented Model Component Library for Constructing Multi-Disciplinary Aircraft Dynamics Models. In *International Forum on Aeroelasticity and Structural Dynamics*, IF-045. CEAS/DLR/AIAA.

Poussot-Vassal, C. (2011). An Iterative SVD-Tangential Interpolation Method for Medium-Scale MIMO Systems Approximation with Application on Flexible Aircraft. In *Proceedings of the 50th IEEE Conference on Decision and Control - European Control Conference*, 7117–7122. Orlando, Florida, USA.

Poussot-Vassal, C. and Vuillemin, P. (2012). Introduction to MORE: a MOdel REduction Toolbox. In *Proceedings of the IEEE Multi-conference on Systems and Control*, 776–781. Dubrovnik, Croatia.

Vuillemin, P., Poussot-Vassal, C., and Alazard, D. (2013). $\mathcal{H}_2$ optimal and frequency limited approximation methods for large-scale LTI dynamical systems. In *Proceedings of the 6th IFAC Symposium on Systems Structure and Control*, 719–724. Grenoble, France.

Vuillemin, P., Poussot-Vassal, C., and Alazard, D. (2014). Poles Residues Descent Algorithm for Optimal Frequency-Limited $\mathcal{H}_2$ Model Approximation. In *Proceedings of the European Control Conference*. Strasbourg, France.